Aust. J. Phys., 1975, **28**, 45–56

Measurement of Apparent Spin–Spin Relaxation Times in Nuclear Quadrupole Resonance using a Double Pulsed Super-regenerative Oscillator

K. R. Doolan[A] *and S. Hacobian*[B]

[A] Department of Physical Chemistry, University of Sydney, Sydney, N.S.W. 2006.
[B] School of Physics, University of New South Wales, Kensington, N.S.W. 2033.

Abstract

A super-regenerative oscillator has been used to obtain apparent spin–spin relaxation times T_2^* for nuclear quadrupole resonance signals from some polycrystalline compounds. A mathematical analysis is given to show how T_2^* values may be obtained from a double pulsed super-regenerative oscillator for both logarithmic and linear modes of detection; each of these modes is described. Results obtained from both modes of operation are examined.

Introduction

In a previous publication (Doolan and Hacobian 1973) we have described the detection of nuclear quadrupole resonance (n.q.r.) using a super-regenerative oscillator (SRO) that is quenched externally by a double pulse signal. The present paper provides a more complete analysis of this method of detection to show how apparent spin–spin relaxation times T_2^* may be evaluated. Before proceeding with this analysis, the operation of the SRO is examined to explain what is meant by linear and logarithmic modes of detection. The changes in T_2^* with impurity concentration in solid mixtures of *p*-dichlorobenzene will be examined in a subsequent communication.

Super-regenerative Oscillator

Spectrometer

A block diagram of the spectrometer used to record n.q.r. signals is given in Fig. 1. The SRO designed to obtain T_2^* values is shown schematically in Fig. 2 and is a modified form of a circuit published by Narath *et al.* (1964). The SRO arrangement used here is cheaper and easier to construct than the spin-echo apparatus employed by other workers (e.g. Bloom *et al.* 1955; Woessner and Gutowsky 1963). Also, the high frequency stability required for the RF oscillator in the spin-echo technique is not necessary when using the SRO. The quench and oscillator tubes V_2 and V_1 of Fig. 2 were taken from separate valves to avoid any interelectrode interference that may arise from using the twin triodes of one glass envelope. The SRO was frequency modulated with a 30 Hz square wave signal applied to a TRW PG 222 variable capacitance diode (varicap) with a +40 V reverse bias. Other workers (Dixon and Bloembergen 1964; Caldwell 1973) have reported that amplitude modulation results when varicaps are used to obtain frequency modulation and have proposed methods to eliminate it. Although amplitude modulation was obtained with the SRO of Fig. 2, it was reduced to a negligible level by adjustment of the trimmer capacitors in the tuned circuit and careful choice of the other components.

The quench signal, shown schematically in Fig. 3, consisted of a train of negative pulses of amplitude -10 V supplied by a Philips modular pulse generator to the quench input of the SRO. This train of pulses is inverted at the plate of V_2 so that the grid of V_1 is at earth potential during the quench pulses and RF oscillations build up exponentially (Frink 1938; Whitehead 1950) from noise and/or any signal in the tuned circuit. Between quench pulses the grid of V_1 is at about -30 V and V_1 is cut off, damping out the RF oscillations.

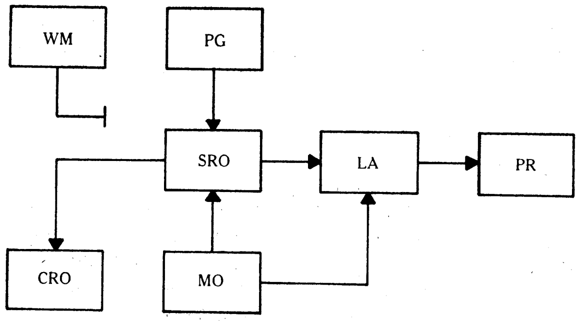

Fig. 1. Block diagram of the n.q.r. spectrometer:
WM, loosely coupled wavemeter; PG, Philips modular pulse generator model PM5720/40; SRO, super-regenerative oscillator; LA, lock-in amplifier; PR, pen recorder; CRO, oscilloscope for display of RF pulses; MO, modulation oscillator.

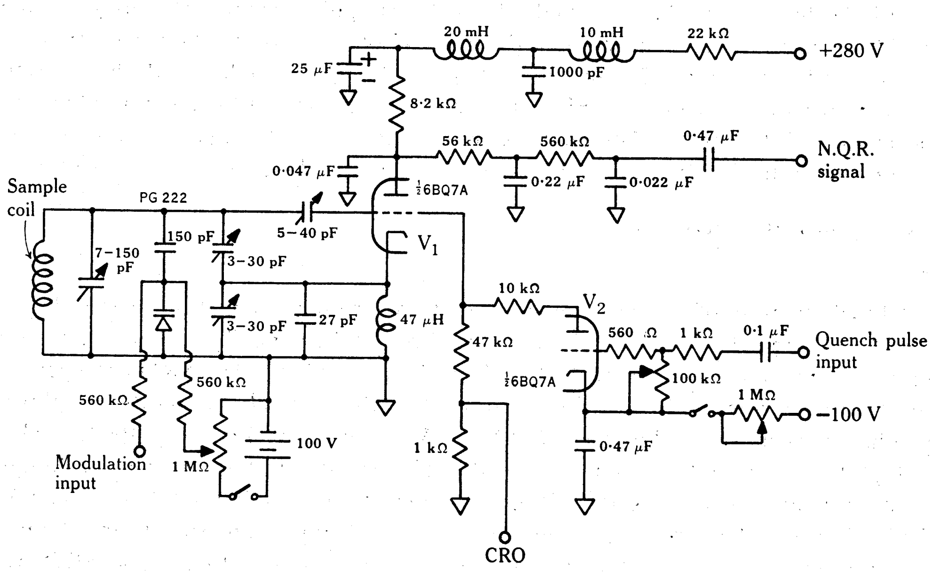

Fig. 2. Circuit diagram of the SRO.

When the rise time of the quench pulses was very fast the high frequency components of the rise time induced RF buildup in the SRO tuned circuit so that the RF pulses were generated from these HF components rather than n.q.r. Results for the variation of n.q.r. signal amplitude at the pen recorder output versus quench pulse rise time are given in Fig. 4, for the experimental conditions described. In all experiments to determine relaxation times the quench pulse rise time was kept fixed at 3 μs.

RF Pulse Area Increase

An SRO is essentially a c.w. oscillator that is periodically turned off by a quench signal which damps out RF oscillations, as explained in the previous subsection. The RF pulses build up exponentially from noise and/or any signal at the oscillator frequency in the tuned circuit and, since they build up earlier when initiated by a signal, these pulses have longer durations and increased 'area' (measured in volt-seconds), as shown in Fig. 5. The waveforms of the quench pulse and RF pulse envelope at the grid of V_1 are shown in Fig. 5*b* for the case where the RF pulse reaches equilibrium oscillation. This grid waveform is inverted and amplified at the plate of V_1.

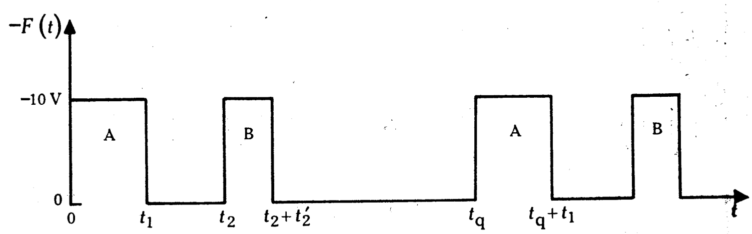

Fig. 3. Schematic representation in the time domain of a double pulse quench signal $F(t)$ with A and B pulses of duration t_1 and t_2' respectively.

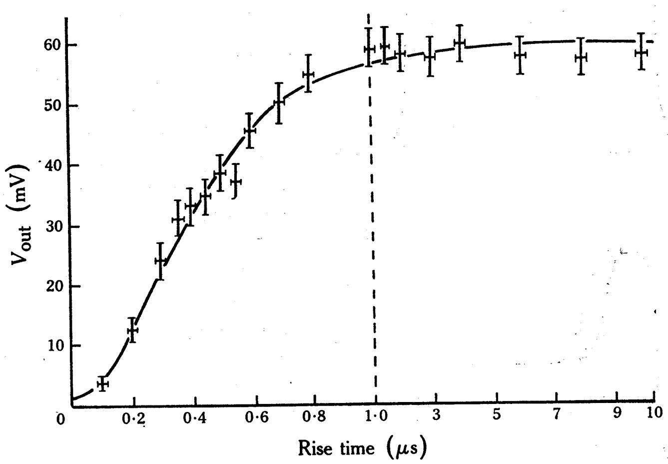

Fig. 4. Dependence of n.q.r. output signal V_{out} on quench pulse rise time. The sample used was *p*-dichlorobenzene at 21°C and the pulse characteristics were $t_q = 1000 \pm 10$ μs, $t_1 = t_2' = 40 \pm 1$ μs and $\tau (= t_2 - t_1) = 30 \pm 1$ μs, with a pulse fall time of 400 ± 10 ns and an SRO frequency of 34·3 MHz.

The time constant of the integrating circuit at the plate of V_1, which consists of a resistor R of 56 kΩ and a capacitor C of 0·22 μF, is approximately 10 ms. For the experiments described here the quench pulses had durations of less than 100 μs so that during a quench pulse the charge on the 0·22 μF capacitor only reached a low level. If V_C and V_R are the voltages across C and R respectively and V_P is the total voltage across C and R then, during a quench pulse,

$$V_P = V_R + V_C \approx iR,$$

since we have $V_C \ll V_R$ and i is the current flow through R. At frequencies greater than 100 Hz most of the current i flows through C so that

$$V_C \approx C^{-1} \int i \, dt \approx (1/RC) \int V_P \, dt. \tag{1}$$

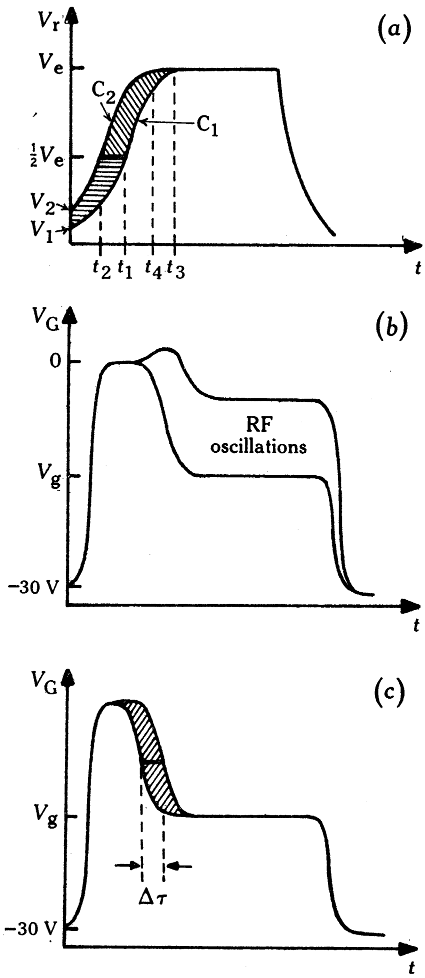

Fig. 5. Waveforms observed in the tuned circuit and at the grid of V_1 of the SRO at equilibrium oscillation:

(*a*) Half of the RF pulse envelope in the tuned circuit when the equilibrium amplitude V_e is reached. V_1 and V_2 are the amplitudes of RF buildup after initiation by noise and noise plus signal respectively, t_2 and t_1 are the times at which the RF pulses have risen to half of their equilibrium level, and t_4 and t_3 are the times at which equilibrium oscillation is reached.

(*b*) RF and quench pulse waveforms observed at the grid of V_1 of Fig. 2 at equilibrium oscillation. As the RF pulse builds up, the grid bias of V_1 becomes more negative, reaching a static value when the pulse attains equilibrium (Whitehead 1950).

(*c*) Grid voltage V_G for two RF pulse leading edges which correspond to two initiating signal amplitudes in the tuned circuit; $\Delta\tau$ is called the time of advance. The complete RF pulse envelopes are not shown.

Let V_P be equal to GV_G, where V_G is the grid waveform of Fig. 5*c* and G is the voltage gain of the circuit. It is not necessary to take the DC voltage at the plate of V_1 into account because there is a capacitor between the output of the SRO and the lock-in amplifier. During an RF pulse it will be assumed that there are many oscillations so that it is only necessary to consider the pulse envelope when evaluating its area. Consequently the voltage across C during a quench pulse is determined by the pulse envelope of Fig. 5*c* and

$$V_C \approx (G/RC) \int V_G \, dt. \tag{2}$$

The voltage across C is proportional to the area under the function V_G. When a signal is detected the RF pulses will build up earlier and equation (2) will have the form

$$V_C' \approx (G/RC) \int V_G' \, dt, \tag{3}$$

where V_C' and V_G' represent the new values of V_C and V_G.

If the SRO is frequency modulated by a low frequency square wave signal with a mark space ratio of 1, half of the quench pulses which occur during a modulation cycle and can detect a signal, will detect one signal level, while the other half will detect another signal level. From equations (2) and (3) the difference in output signal across the capacitor C between consecutive half-modulation cycles for the above modulation signal is given by

$$\frac{nt_m}{2t_q}(V_C' - V_C) = \frac{nt_m G}{2t_q RC} \int (V_G' - V_G) \, dt, \tag{4}$$

where $nt_m/2t_q$ is the number of quench pulses per half modulation cycle which can detect a signal, t_m and t_q being the modulation and quench periods respectively and n the number of pulses per quench period which can detect a signal. For double pulse detection of n.q.r. the value of n is 1. The output signal voltage V_{out} at the pen recorder of Fig. 1 is given by

$$V_{out} = k_1(nt_m G/2t_q RC)\Delta A_g, \tag{5}$$

where ΔA_g is the area increase of the grid waveform, and represents the integral of equation (4), and k_1 is a constant for constant gain of the pen recorder and lock-in amplifier. Equation (5) may be written in the form

$$V_{out} = k_2 \Delta A_g / t_q, \tag{6}$$

where k_2 is constant if k_1, n, t_m and G are all kept constant.

Logarithmic Mode

In the logarithmic mode of operation RF oscillations build up to an equilibrium amplitude when the supply of energy by the valve V_1 is equal to the loss of energy from the tuned circuit. As in Fig. 5*a*, let t_4 and t_3 be the times at which equilibrium oscillation of a particular RF pulse is reached when different signal amplitudes initiate RF buildup. The difference $t_3 - t_4 = \Delta\tau$ is called the time of advance of the RF pulse due to increase in signal amplitude at the tuned circuit.

The diagram in Fig. 6 of the envelope of the RF pulse buildup in the SRO tuned circuit was obtained by tracing an oscilloscope display onto a sheet of polythene fixed to the screen of the oscilloscope. To obtain this display, a coil consisting of three turns of gauge 16 copper wire and having twice the diameter of the sample coil was placed coaxially with the sample coil so that the centres of the two coils were about 5 cm apart. The RF oscillations induced in this coil were displayed on a Tektronix 7704 oscilloscope.

Let an RF pulse in the tuned circuit building up from noise reach a voltage V_1 at $t = 0$, $\frac{1}{2}V_e$ at t_1 and V_e at t_3, as shown in Fig. 5*a*. Similarly, let a pulse building up from noise and signal reach an amplitude V_2 at $t = 0$, $\frac{1}{2}V_e$ at t_2 and V_e at t_4. The voltages V_1 and V_2 are related to the initiating voltages by (Frink 1938; Whitehead 1950)

$$V_1 = \rho\langle V_n^2\rangle^{\frac{1}{2}}, \qquad V_2 = \rho(\langle V_n^2\rangle + \langle V_s^2\rangle)^{\frac{1}{2}}, \tag{7}$$

where ρ is the voltage gain up to the time $t = 0$, $\langle V_n^2\rangle$ is the mean square noise voltage at the tuned circuit and $\langle V_s^2\rangle$ is the mean square signal voltage that initiates

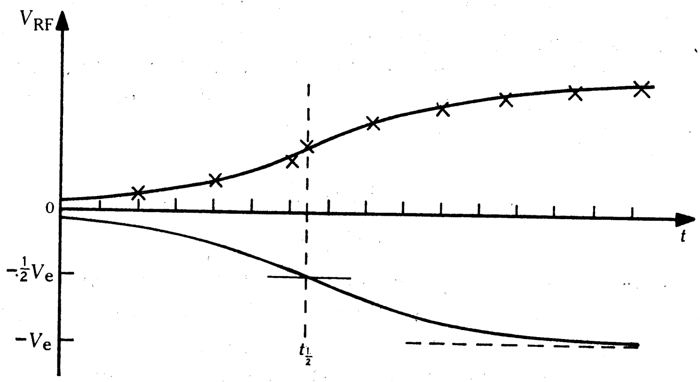

Fig. 6. Initial RF pulse buildup to equilibrium, as traced from an oscilloscope display. V_{RF} is the pulse amplitude and one division on the time axis represents $0 \cdot 2\ \mu$s. At time $t_{\frac{1}{2}}$ the pulse has reached half its equilibrium level. The crosses were plotted using (with $a = 0 \cdot 70\ \mu$s)

$$\begin{array}{ll} V_1 \exp(t/a) & \text{for} \quad t < t_{\frac{1}{2}}, \\ \frac{1}{2}V_e + \frac{1}{2}V_e(1 - \exp\{-(t-t_{\frac{1}{2}})/a\}) & \text{for} \quad t \geqslant t_{\frac{1}{2}}. \end{array}$$

RF buildup at an earlier time in the tuned circuit. The area bounded by the curves C_1 and C_2 of Fig. 5*a* is equal to the sum of an infinite number of trapezia each with base $\Delta\tau$ and infinitesimal height. This sum is given by

$$\Delta A = \Delta\tau\, V_e,$$

since the area of a trapezium is equal to the base length multiplied by its perpendicular height. Similarly, the area increase of the grid waveform, ΔA_g, is $\Delta\tau\, V_g$, where V_g is defined in Fig. 5*c*. Substitution of these results into equation (6) gives

$$V_{out} = k_3 \Delta\tau\, V_e/t_q = k_3 \Delta A/t_q, \tag{8}$$

where $k_3 = k_2 V_g/V_e$ is constant for a particular SRO with constant operating conditions.

The area increase ΔA is calculated as follows. As in Fig. 6, RF buildup to $\frac{1}{2}V_e$ is given by the function $\exp(t/a)$, while the buildup between $\frac{1}{2}V_e$ and V_e is given by

$$\tfrac{1}{2}V_e + \tfrac{1}{2}V_e\{1 - \exp(-(t-t_{\frac{1}{2}})/a)\}.$$

Let the area between the curves C_1 and C_2 below $\frac{1}{2}V_e$ in Fig. 5*a* be ΔA_1 and that above $\frac{1}{2}V_e$ be ΔA_2. Then

$$\Delta A_1 = V_2 \int_0^{t_2} \exp(t/a)\, dt + \tfrac{1}{2}V_e(t_1 - t_2) - V_1 \int_0^{t_1} \exp(t/a)\, dt,$$

that is,

$$\Delta A_1 = a(V_1 - V_2) + \tfrac{1}{2}aV_e \ln(V_2/V_1). \tag{9}$$

Similarly,

$$\Delta A_2 = \tfrac{1}{2}V_e \int_{t_2}^{t_4} \{2 - \exp(-(t-t_2)/a)\}\, dt + V_e(t_3 - t_4) - \tfrac{1}{2}V_e(t_1 - t_2)$$

$$-\tfrac{1}{2}V_e \int_{t_1}^{t_3} \{2 - \exp(-(t-t_1)/a)\}\, dt$$

$$= \tfrac{1}{2}V_e(t_1 - t_2) + \tfrac{1}{2}aV_e\{\exp(-(t_4 - t_2)/a) - \exp(-(t_3 - t_1)/a)\}. \tag{10a}$$

Since $t_4 - t_2 = t_3 - t_1$, equation (10a) reduces to

$$\Delta A_2 = \tfrac{1}{2}aV_e \ln(V_2/V_1). \tag{10}$$

Combining equations (9) and (10), the total area increase is given by

$$\Delta A = \Delta A_1 + \Delta A_2 \approx aV_e \ln(V_2/V_1), \tag{11}$$

because V_1 and V_2 are of the order of the initiating voltages and are small compared with V_e. Substituting for V_2 and V_1 from equations (7) we then have

$$\Delta A \approx aV_e \ln\{(\langle V_s^2\rangle + \langle V_n^2\rangle)/\langle V_n^2\rangle\}^{\frac{1}{2}}, \tag{12}$$

and thus from equation (8)

$$V_{\text{out}} = \frac{k_3 a V_e}{t_q} \ln\left(\frac{\langle V_s^2\rangle + \langle V_n^2\rangle}{\langle V_n^2\rangle}\right)^{\frac{1}{2}}. \tag{13}$$

Equation (13) relates the output voltage at the pen recorder to the RF signal voltage in the tuned circuit of the SRO when the RF pulses reach equilibrium oscillation. This equation also holds for a diode detector which is loosely coupled to the sample coil. For a particular value V_x of V_{out}, for which $\Delta\tau = \Delta\tau_x$, equation (8) may be written as

$$V_x = k_3 \Delta\tau_x V_e/t_q \qquad \text{or} \qquad k_3 = V_x t_q/\Delta\tau_x V_e. \tag{14a, b}$$

Substituting equation (14b) into (13), we have

$$V_{\text{out}} = \frac{aV_x}{\Delta\tau_x} \ln\left(\frac{\langle V_s^2\rangle + \langle V_n^2\rangle}{\langle V_n^2\rangle}\right)^{\frac{1}{2}}. \tag{15}$$

To measure $\Delta\tau_x$ for the circuit of Fig. 2, the buildup of the RF pulses was displayed on a Tektronix 7704 oscilloscope while the SRO was detecting a signal generated by an RF oscillator. For square wave modulation, the pulse envelopes alternated between two values corresponding to the two signal amplitudes which were initiating RF buildup in the SRO tuned circuit. The leading edges of the RF pulses alternated between two well-defined positions separated by the interval $\Delta\tau_x$. At the same time that $\Delta\tau_x$ was measured, the corresponding output voltage V_x at the pen recorder was noted. All of the RF pulses of the SRO detected the signal from the RF generator. For double pulse quenching, t_q was made long enough so that only half of the pulses were able to detect n.q.r. and, as a result, the value of V_x required was half of the peak to peak output voltage. The values of V_e and t_q were also measured from the oscilloscope display. The value of k_3 was found by substituting results for V_e, t_q, $\Delta\tau_x$ and V_x into equation (14b). The time constant a of RF buildup was determined as indicated in Fig. 6 by fitting a curve of the form $\exp(t/a)$ to the pulse buildup.

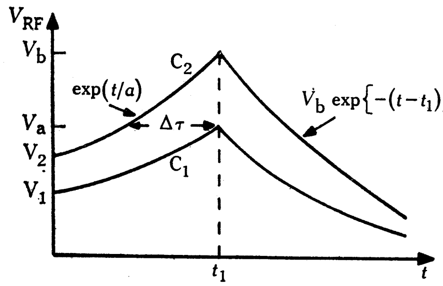

Fig. 7. Half RF pulse envelope V_{RF} when oscillation is damped out well below equilibrium. Curve C_1 builds up to V_a at time t_1 from noise while C_2 builds up to V_b at t_1 from noise plus signal.

Linear Mode

In the linear mode of operation, RF oscillations are damped out well before equilibrium is reached. Oscillations build up and decay exponentially (Frink 1938; Whitehead 1950) with respect to time, as shown in Fig. 7. The RF pulses at the grid of V_1 and in the SRO tuned circuit have the same buildup envelope, and the pulse area increase at the plate of V_1 is given by a constant times the area between curves C_1 and C_2 of Fig. 7 up to the time t_1, that is,

$$\Delta A = \int_0^{t_1} V_2 \exp(t/a)\,\mathrm{d}t - \int_0^{t_1} V_1 \exp(t/a)\,\mathrm{d}t$$

$$= a(V_2 - V_1)\{\exp(t_1/a) - 1\}. \tag{16}$$

Substitution of this expression into equation (6) gives

$$V_{\text{out}} = (k_2'\,a/t_q)(V_2 - V_1)\{\exp(t_1/a) - 1\}$$

and thus, using equations (7),

$$V_{\text{out}} = (k_4/t_q)\{(\langle V_s^2\rangle + \langle V_n^2\rangle)^{\frac{1}{2}} - \langle V_n^2\rangle^{\frac{1}{2}}\}, \tag{17}$$

where $k_4 = \rho a k_2'\{\exp(t_1/a) - 1\}$ is a constant for a particular SRO with fixed operating conditions. For $\langle V_s^2\rangle \gg \langle V_n^2\rangle$ equation (17) reduces to

$$V_{\text{out}} = (k_4/t_q)\langle V_s^2\rangle^{\frac{1}{2}}. \tag{18}$$

If diode detection is used, similar equations to (17) and (18) result but ΔA is taken as the area between the curves C_1 and C_2 of Fig. 7 and is evaluated by integrating over all values of t.

Measurement of T_2^*

If an SRO is quenched with the double pulse train shown in Fig. 3, pairs of RF pulses occur in the tuned circuit. All of these pulses can excite n.q.r., but if the repetition time t_q of the double pulse train is long compared with the value of the apparent spin–spin relaxation time T_2^* for the sample that is being excited, the nuclear induction signal from a pair of pulses will have decayed well below noise at the arrival of the next pair. For this condition only the second pulses (B pulses) of each pair will detect the induction signal produced by the first (A) pulses of each pair. Thus if $t_q \gg T_2^*$ and $\tau = t_2 - t_1$ is long enough to allow the RF pulses A to decay well below noise before the buildup of the B pulses begins, the response of the SRO to an n.q.r. signal is given by equation (15) when the B pulses reach equilibrium and by equation (17) when they are damped out well below equilibrium. (If τ is not long enough to allow this, $\langle V_s^2\rangle$ is replaced by $\langle V_s^2 + V_a^2\rangle$ in equation (7), where V_a is the amplitude of the RF pulse A which initiates the buildup of pulse B. Consequently in the present work τ was kept greater than 20 μs to avoid taking V_a into account.)

It has been shown for n.q.r. (Bloom *et al.* 1955) that the average components of the nuclear spin I of a sample after irradiation by an RF pulse in zero static magnetic field are given by

$$\langle I_x\rangle = \tfrac{1}{2}\xi^{\frac{1}{2}}\sin(\xi^{\frac{1}{2}}\gamma B_1 t_1)\sin\{\omega_0(t-t_1)\}\exp\{-((t-t_1)/T_2^*)^2\} \tag{19a}$$

and

$$\langle I_y\rangle = \langle I_z\rangle = 0\,, \tag{19b}$$

where

$$\xi = (I+|m|)(I-|m|+1)\,,$$

m being the z component of I. In equation (19a), γ is the magnetogyric ratio of the nuclei undergoing n.q.r., B_1 is the amplitude of the RF magnetic field, t is the time, t_1 is the duration of the RF pulse and ω_0 is the radio frequency (of the SRO). The apparent spin–spin relaxation time T_2^* is taken to be the time for the induction signal from the sample after one RF pulse to decay to e^{-1} times its maximum value. It should be noted that the quantities t_w and δ used by Bloom *et al.* (1955) are related to t_1 and T_2^* by $t_1 = t_w$ and $T_2^* = 2/\delta$. For a single crystal in zero static magnetic field, the total magnetization M induced in the sample by an RF pulse is given by $M = \gamma\hbar n\langle I_x\rangle$, where n is the total number of nuclei which have been excited. For a polycrystalline sample B_1 is replaced by $B_1\sin\theta$ (Bloom *et al.* 1955) and M is averaged with respect to θ, the angle between B_1 and the axis of quantization of I.

The magnetization M produces a magnetic induction B equal to $\mu_0 M$ in free space (MKS units). As in Bloch's (1946) paper, the flux Φ produced by B through the receiver coil of N turns containing a sample of cross sectional area A is given by

$$\Phi = \mu_0 NAM\,,$$

assuming the sample has a constant cross sectional area over the length of the coil.

The signal voltage V_s induced in the receiver coil is determined by (in MKS units)

$$V_s = -\mathrm{d}\Phi/\mathrm{d}t = -\mu_0 NA\,\mathrm{d}M/\mathrm{d}t.$$

Substitution of equation (19a) into this expression, with $\tau = t - t_1$, gives

$$V_s = -\tfrac{1}{2}\mu_0 NA\gamma\hbar n\xi^{\frac{1}{2}}\omega_0 \sin(\xi^{\frac{1}{2}}\gamma B_1 t_1)$$
$$\times\left[\cos(\omega_0\tau)\exp\left\{-\left(\frac{\tau}{T_2^*}\right)^2\right\} - \frac{2\tau}{\omega_0(T_2^*)^2}\sin(\omega_0\tau)\exp\left\{-\left(\frac{\tau}{T_2^*}\right)^2\right\}\right]. \tag{20}$$

For the experimental work reported here $2\tau/(T_2^*)^2$ is much less than ω_0 for all values of τ used. Therefore the second term of equation (20) is neglected and, for a polycrystalline sample or single crystal, the mean square signal voltage induced in the sample coil may be written in the form

$$\langle V_s^2\rangle = D^2\exp\{-2(\tau/T_2^*)^2\}, \tag{21}$$

where D is a constant if N, A, ξ, n, γ, B_1, t_1 and ω_0 are all held constant. This is possible if each of the RF pulses applied to the sample has fixed amplitude and duration, the RF frequency is constant and the sample has a fixed mass and occupies a constant volume in the given sample coil.

Logarithmic Mode

Substituting equation (21) into (15), we have

$$V_{\mathrm{out}} = \frac{aV_x}{2\,\Delta\tau_x}\ln\left(\frac{D^2\exp\{-2(\tau/T_2^*)^2\} + \langle V_n^2\rangle}{\langle V_n^2\rangle}\right).$$

Rearranging this expression, taking natural logarithms and putting $b = (aV_x/2\,\Delta\tau_x)$, gives

$$-2(\tau/T_2^*)^2 = \ln\{\exp(V_{\mathrm{out}}/b) - 1\} + \ln\{\langle V_n^2\rangle/D^2\}. \tag{22}$$

Equation (22) shows that, for logarithmic mode detection, the gradient of a graph of $\ln\{\exp(V_{\mathrm{out}}/b) - 1\}$ against τ^2 is $-2/(T_2^*)^2$, from which T_2^* can be evaluated.

Linear Mode

Substituting equation (21) into (17), we have

$$V_{\mathrm{out}} = (k_4/t_q)\left[\{\langle V_n^2\rangle + D^2\exp(-2(\tau/T_2^*)^2)\}^{\frac{1}{2}} - \langle V_n^2\rangle^{\frac{1}{2}}\right].$$

Rearranging this expression and taking natural logarithms gives

$$-2(\tau/T_2^*)^2 = \ln\{(V_{\mathrm{out}}t_q/k_4 + \langle V_n^2\rangle^{\frac{1}{2}})^2 - \langle V_n^2\rangle\} - 2\ln D. \tag{23}$$

If we have $\langle V_s^2\rangle \gg \langle V_n^2\rangle$, equation (23) reduces to

$$-(\tau/T_2^*)^2 \approx \ln(V_{\mathrm{out}}t_q/k_4) - \ln D. \tag{24}$$

Equation (23) is difficult to apply because $\langle V_n^2\rangle$ must be determined before T_2^* can be evaluated. However, for $\langle V_s^2\rangle \gg \langle V_n^2\rangle$, the gradient of a graph of $\ln V_{\mathrm{out}}$ against τ^2 is $-(T_2^*)^{-2}$.

Results

Logarithmic Mode

Using double pulse quenching the result of Fig. 8 was obtained for fused *p*-dichlorobenzene and the experimental conditions listed. For logarithmic-mode detection, the second RF pulse (B) of each pair was allowed to build up to equilibrium oscillation so that equation (22) described the SRO response to an n.q.r. signal. The results of Table 1 were obtained from graphs similar to Fig. 8. For each determination, t_q was made large enough so that no signal was detected at the pen recorder for $\tau = \frac{1}{2}t_q$.

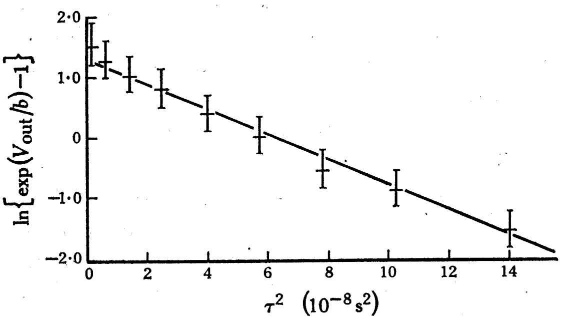

Fig. 8. Graph for determination of T_2^* for ^{35}Cl n.q.r. in fused *p*-dichlorobenzene at 25°C. The pulse sequence was $t_1 = 40\pm1$ μs (A pulse), $t_2' = 12\pm1$ μs (B pulse) and $t_q = 1000\pm10$ μs, and the SRO frequency was 34·3 MHz. The experimental value of b was 40 ± 5 mV. The result of the measurement was $T_2^* = 310\pm15$ μs.

Table 1. T_2^* values obtained using SRO

The SRO of Fig. 2 with double pulse quenching was used for the n.q.r. of the polycrystalline compounds listed. In all measurements t_1 and t_2' were 40 ± 1 and 12 ± 1 μs respectively. The results were obtained from graphs similar to Fig. 8

Nucleus	Compound	Temp.	ω_0 (MHz)	t_q (μs)	T_2^* (μs)
^{35}Cl	*p*-dichlorobenzene	25°C	34·3	1000	310 ± 15
		81 K	34·8	1000	205 ± 10
^{37}Cl	*p*-dichlorobenzene	23°C	27·1	1000	350 ± 30
		81 K	27·4	1000	240 ± 20
^{35}Cl	$NaClO_3$	23°C	30·0	1000	330 ± 30
	$SbCl_3$	31°C	19·0	1000	200 ± 15
	$SbCl_3$	31°C	20·4	1000	180 ± 20
^{63}Cu	Cu_2O	25°C	26·0	300 ± 4	34 ± 3
^{65}Cu	Cu_2O	27°C	24·1	200 ± 4	30 ± 3

The results in Table 1 may be compared with the T_2^* values of 310 and 230 μs for ^{35}Cl n.q.r. in *p*-dichlorobenzene at room temperature and 77 K respectively, obtained by Woessner and Gutowsky (1963) using the spin-echo technique. They also found the ^{63}Cu n.q.r. signal at room temperature to have a T_2^* value of about 30 μs. No error estimates were given. Bloom *et al.* (1955) obtained an experimental value of $T_2^* \sim 0{\cdot}3$ ms for ^{35}Cl n.q.r. at room temperature in polycrystalline $NaClO_3$, also using the spin-echo technique.

In the present work, the T_2^* values for ^{37}Cl n.q.r. in *p*-dichlorobenzene were found to be significantly higher than those obtained for ^{35}Cl, indicating that the ^{35}Cl and ^{37}Cl nuclei interact differently with the crystal lattice. The T_2^* values for ^{35}Cl and

^{37}Cl in fused *p*-dichlorobenzene were found to be lower at 81 K than at room temperature, presumably due to strains or other imperfections (Woessner and Gutowsky 1963) arising in the crystal lattice when it was cooled. The strong and weak ^{35}Cl n.q.r. lines of polycrystalline $SbCl_3$ gave the same T_2^* value within experimental error, as also did the n.q.r. lines of ^{63}Cu and ^{65}Cu in powdered Cu_2O at room temperature.

Linear Mode

For linear-mode detection using double pulse quenching, the A pulses were allowed to reach equilibrium and were made long to excite as many nuclei as possible. The B pulses were made short enough ($\sim 0\cdot5\ \mu s$) to ensure that RF oscillations were damped out well below equilibrium and their response to an n.q.r. signal was in the linear mode. As for the logarithmic mode, t_q was made sufficiently long so that no signal was detected by the pen recorder at $\tau = \frac{1}{2}t_q$.

Using equation (24) and assuming $\langle V_s^2 \rangle \gg \langle V_n^2 \rangle$, estimates of T_2^* were obtained from graphs of $\ln V_{out}$ against τ^2. The resulting values of T_2^* from this method were: $230 \pm 10\ \mu s$ for ^{35}Cl in fused *p*-dichlorobenzene at 24°C, $220 \pm 20\ \mu s$ for ^{35}Cl in polycrystalline $NaClO_3$ at 23°C, and $240 \pm 10\ \mu s$ for ^{37}Cl in fused *p*-dichlorobenzene at 25°C. (The pulse sequence used was $t_1 = 40 \pm 1\ \mu s$, $t_2' = 0\cdot5 \pm 0\cdot2\ \mu s$ and $t_q = 1000 \pm 10\ \mu s$.) These T_2^* values are much lower than those obtained from the logarithmic-mode analysis and by the spin-echo technique (Bloom *et al.* 1955; Woessner and Gutowsky 1963). This indicates that the assumption $\langle V_s^2 \rangle \gg \langle V_n^2 \rangle$ is incorrect for the experimental conditions used here. Since $\langle V_n^2 \rangle$ is difficult to measure, equation (23) was not applied.

Acknowledgments

One of us (S.H.) gratefully acknowledges assistance from the Australian Research Grants Committee. We both wish to thank Mr L. Klososzczyk for advice about electronics.

References

Bloch, F. (1946). *Phys. Rev.* **70**, 460.
Bloom, M., Hahn, E. L., and Herzog, B. (1955). *Phys. Rev.* **97**, 1699.
Caldwell, R. A. (1973). *Aust. J. Chem.* **26**, 1611.
Dixon, R. W., and Bloembergen, N. (1964). *J. Chem. Phys.* **41**, 1720.
Doolan, K. R., and Hacobian, S. (1973). *Aust. J. Chem.* **26**, 859.
Frink, F. W. (1938). *Proc. Inst. Radio Eng.* **26**, 76.
Narath, A., O'Sullivan, W. J., Robinson, W. A., and Simmons, W. W. (1964). *Rev. Sci. Instrum.* **35**, 476.
Whitehead, J. R. (1950). 'Super-regenerative Receivers' (Cambridge Univ. Press).
Woessner, D. E., and Gutowsky, H. S. (1963). *J. Chem. Phys.* **39**, 440.

Manuscript received 25 July 1974